**Aspden AJ.**

**A numerical study of diffusive effects in turbulent lean premixed hydrogen flames.**

***Proceedings of the Combustion Institute,* 2016**

**DOI: http://dx.doi.org/10.1016/j.proci.2016.07.053**

# A Numerical Study of Diffusive Effects in Turbulent Lean Premixed Hydrogen Flames

A. J. Aspden[1]

[1] *Mathematical Sciences, University of Southampton, Southampton, Hampshire, SO17 1BJ, UK*

**Abstract**

Three-dimensional direct numerical simulation of lean premixed hydrogen flames is used to explore the influence of species and thermal diffusion and viscosity on the flame structure and turbulent flame response. The leading-order flame response is shown to be due to the global Lewis number with little influence from the other species. The previously-reported observation of decorrelation of fuel consumption and heat release at high Karlovitz numbers is shown to be solely due to atomic hydrogen diffusion. Finally, it is shown that the suppression of turbulence through the flame cannot be attributed to an increase in viscosity due to the increase in temperature, but that the effect is not negligible. It is further argued that turbulence-flame interactions are better described considering Kolmogorov's second similarity hypothesis (rather than the first); specifically, by a Karlovitz number that is defined based on the inertial subrange (i.e. the energy dissipation rate) rather than the dissipation subrange (i.e. viscosity or equivalently Kolmogorov scale quantities).

*Keywords:* Turbulent premixed flames, direct numerical simulation, detailed chemistry, low Mach number flow, hydrogen

## 1. Introduction

Three-dimensional direct numerical simulation (DNS) of turbulent combustion with detailed chemistry and transport is an important tool for understanding the fundamentals of turbulent premixed flames and for developing and validating turbulent flame models. There is a growing body of work using DNS with detailed kinetics to study the canonical flame-in-a-box configurations examining a wide range of fuels and conditions; examples include [1–3] in hydrogen, [4–6] in methane, and [7, 8] in heavier fuels like heptane and dodecane. A common theme that comes out of this work is the importance of the global Lewis number (the Lewis number of the deficient species) and how its influence is moderated (or enhanced) by turbulence, but it is becoming increasingly clear that there are secondary effects that cannot be explained by the global Lewis number, e.g. the decorrelation of fuel consumption rate and heat release observed in [9, 10]. A unique advantage of DNS with detailed chemistry is that subtle artificial changes can be made to transport properties to attribute observed phenomena to specific properties of the fuel and/or turbulence. The present paper presents such a study, using lean premixed hydrogen flames at moderate turbulence levels to investigate the effects of Lewis number of both molecular and atomic hydrogen in particular, and also to investigate the effect of the increase in viscosity across the flame as the temperature increases.

Turbulence is characterised using the ratios of time scales, see [11], for example. Specifically, the Damköhler number is defined as the ratio of the fluid time scale at the integral length $\tau_u = l/u$ to the flame time scale $\tau_F = l_F/s_F$

$$\mathrm{Da} = \frac{\tau_u}{\tau_F} = \frac{s_F}{\check{u}}\frac{l}{l_F}, \qquad (1)$$

where $\check{u}$ and $l$ are the turbulent rms velocity fluctuation and integral length scale, respectively, and $s_F$ and $l_F$ are the flame speed and width, respectively. Note that freely-propagating values for $s_F$ and $l_F$ have been used to account for the thermodiffusive unstable nature of lean premixed hydrogen flames [12]. The Karlovitz number can be defined as the ratio of flame time scale to the Kolmgorov time scale $\tau_\eta = \eta/u_\eta$

$$\mathrm{Ka}_\eta^2 = \left(\frac{\tau_F}{\tau_\eta}\right)^2 = \mathrm{Re}_F\left(\frac{\check{u}^3}{s_F^3}\frac{l_F}{l}\right), \qquad (2)$$

where $\mathrm{Re}_F = s_F l_F/\nu$ is the flame Reynolds number, which is often taken unity (although actual values can be an order of magnitude greater or smaller; $\mathrm{Re}_F \approx 10.5$ here). Assuming that the inertial range extends down to approximately $\beta\eta$, where $\beta$ is some factor, (e.g. $\beta \approx 10$, see [13, 14]), then scales comparable with the flame thickness are in the inertial range when $l_F \gtrsim \beta\eta$, which can be shown to be equivalent to $\mathrm{Ka}_\eta \gtrsim \beta^2 \mathrm{Re}_F^{-3/2}$, which is approximately 3 here (for $\beta \approx 10, \mathrm{Re}_F \approx 10.5$). That means even for moderate $\mathrm{Ka}_\eta$, the flame thickness is in the inertial subrange, and so defining a Karlovtiz number in terms of Kolmgorov scales is questionable. By the second similarity hypothesis, viscosity is unimportant, and it is the energy dissipation rate $\varepsilon = u^3/l$ that is the appropriate measure. Consequently, *defining* the Karlovtiz number to be

$$\mathrm{Ka}_\varepsilon^2 = \frac{\check{u}^3}{s_F^3}\frac{l_F}{l}, \qquad (3)$$

is a more appropriate characterisation of turbulence-flame interactions than equation (2) as it is characteristic of the inertial subrange rather than the dissipation subrange. Simulations will be presented in section 3.3 that lend further support to this argument.

In the present paper, simulations at $\mathrm{Ka}_\varepsilon = 12$ and 36 are presented (following equation 3) and $\Lambda = l/l_F = 1$, which are designed to be consistent with the simulations presented in [6, 10] at $\Lambda = 4$. All of the simulations presented here involve lean premixed hydrogen flames at an equivalence ratio of $\varphi = 0.4$, which has a global Lewis number of approximately 0.35 making the flames thermodiffusively unstable. The diffusive processes are examined by artificially changing diffusion coefficients. While this is unphysical and unrealistic, it is a purely numerical approach that provides insight into the relative importance of different diffusive processes in the flame, highlighting the root causes of turbulent flame response.

The study is divided into three parts: first, scalar diffusion processes are examined at moderate turbulence intensity ($\mathrm{Ka}_\varepsilon = 12$) with a focus on large-scale flame response at low global Lewis numbers; second, diffusion of atomic hydrogen is specifically considered in a more turbulent flame ($\mathrm{Ka}_\varepsilon = 36$) with a focus on the decorrelation between fuel consumption rate and heat release that was reported in [9, 10]; third, viscous processes are examined at $\mathrm{Ka}_\varepsilon = 12$ with a focus on effects on leading order turbulent statistics through the flame.

## 2. Computational Methodology

The simulations presented here are based on the well-established low Mach number formulation of the reacting flow equations [15]. The fluid is treated as a mixture of perfect gases, and a mixture-averaged model is assumed for diffusive transport, ignoring Dufour and Soret effects. A source term is used in the momentum equation to establish and maintain turbulence with the desired properties [14]. The chemical kinetics and transport are modelled using the Li *et al.* hydrogen mechanism [16], which consists of 9 species with 19 fundamental reactions.

The performance of the scheme for direct numerical simulation of premixed flame systems in regimes comparable to the present study was examined in [14]. An *effective* Kolmogorov length scale was formulated, which measures the actual Kolmogorov length scale realised in a simulation at a given resolu-

tion. Here, the most computationally demanding simulation (with unaltered viscosity), having the highest turbulence levels, has a computational cell width that is approximately 1.8 times the Kolmogorov length scale. At this resolution, the numerical scheme produces an *effective* Kolmogorov length scale that about 8.8% larger than the analytical value in the worst case.

### *2.1. Simulation Configuration*

The simulations were run at atmospheric conditions in a high aspect ratio domain, with periodic lateral boundary conditions, a free-slip base and outflow at the top. The momentum source term that maintains the background turbulence results in a time-dependent zero-mean velocity field. It was shown in [14] that this approach gives approximately 10 integral length scales across the domain width. The freely-propagating [12] flame speed is $s_F \approx 47.4$ cm/s and thermal thickness is $l_F \approx 410$ microns. The forcing term that maintains the turbulence gives rise to an integral length scale that is approximately one tenth of the domain size, and the domain width was chosen such that $L = 4.1$ mm so that $\Lambda = 1$ and $L = 10l = 10l_F$. Although these simulations are smaller than previously reported, the focus here is on small-scale turbulence-flame interactions, and so the domain size is sufficient for the current purposes (a larger domain or integral length scale at the same $\mathrm{Ka}_\varepsilon$ would simply create more flame surface area with essentially the same turbulence-flame interactions). An inert calculation was run to establish the turbulence at reduced expense, and the reacting flow simulation was initialised by superimposing a laminar flame solution onto the turbulent velocity field.

The simulations at $\mathrm{Ka}_\varepsilon = 12$ used a computational grid of $128\times128\times512$, and those at $\mathrm{Ka}_\varepsilon = 36$ used a grid of $192\times192\times768$ to ensure that the smallest turbulence scales were sufficiently well resolved. These resolutions correspond to approximately 13 and 19 computational cells across the thermal thickness, respectively, which is more than adequate for this mechanism [1].

### *2.2. Part I: global Lewis number*

The first part of the study considers modified species diffusion coefficients. Five cases are considered by changing the diffusive coefficients of different species, and a sixth case by modifying thermal diffusion: case Ia is a control simulation with full unaltered transport coefficients; case Ib sets the Lewis number for all species equal to the Lewis number for molecular hydrogen; case Ic sets a unity Lewis number for all species except molecular hydrogen; case Id sets a unity Lewis number for molecular hydrogen, leaving all other coefficients unchanged; case Ie sets a unity Lewis number for all species; case If divides the thermal diffusion coefficient by a factor of ten, leaving all species coefficients unchanged. Each simulation was restarted from a common time point taken from the control simulation after the flame had become established. Modifying the diffusion coefficients affects reference flame quantities, but appropriately reevaluated Karlovitz numbers remain between approximately 11.6 and 14.6, and so all flames will remain in the same combustion regime.

### *2.3. Part II: atomic hydrogen diffusion*

In [9, 10], a decorrelation between fuel consumption rate and heat release was observed, and it was speculated that diffusion of atomic hydrogen was responsible. The second part of the study considers two cases at $\mathrm{Ka}_\varepsilon = 36$ to investigate this suggestion. Specifically, a control case with unaltered diffusion coefficients (case IIa) and a case where just the Lewis number of atomic is changed to unity (case IIb).

### *2.4. Part III: viscosity*

The third part of the study considers modifying viscosity. Reduced levels of turbulence are typically observed downstream of a flame, which is sometimes attributed to the increase of viscosity with increasing temperature (e.g. [7, 17]). The baseline case Ia is used as the control, and five simulations with modified viscosity are considered: case IIIb sets $\mu$ to be a constant (from the unburned side); case IIIc sets $\mu$ to be a constant (from the burned side); case IIId sets $\mu$ to be a constant (reduced by the same factor as the ratio of b and c); case IIIe sets $\nu$ to be a constant (this results in a decrease in viscosity proportional to $\rho$); case IIIf $\mu$ gradually decreases to zero through the flame (as a linear function of $\rho$); case IIIg sets viscosity to be zero everywhere; case IIIh sets viscosity to be zero, along with species and thermal diffusion. The ability to set the viscosity to zero (in cases IIIf-IIIh) is a particular feature of the non-oscillatory finite-volume scheme employed, which remain stable even in the absence of viscous forces; an approach is often referred to as Implicit Large Eddy Simulation (ILES); see [18] and the references therein for a comprehensive review of the technique. The performance of the present numerical scheme when running with zero or underresolved viscosity was examined in [14], which demonstrated that whereas a real-world (constant-temperature) fluid has a fixed viscosity and the Kolmogorov length scale varies depending on the energy dissipation rate at the large scales, an ILES fluid has a fixed effective Kolmogorov length scale and the effective viscosity varies depending on the energy dissipation rate at the large scales. With an appropriate non-dimensionalisation (i.e. using the effective Kolmogorov length scale), the inertial range and onset of the dissipation range of the energy spectra collapse to the same curve as in a real viscous fluid (see figure 4 in [14]); the effective Kolmogorov length scale of the present scheme was shown to be approximately 0.3 computational cell widths.

## 3. Results

### *3.1. Part I: global Lewis number*

Two-dimensional slices through the three-dimensional data for cases Ia-If are shown in figure 1; note periodicity has been exploited to stitch together $x = 0$ and $y = 0$ planes to show more flame surface (each panel is two domain widths across and four high). In each case the panels (left-to-right) are fuel mass fraction, temperature, fuel consumption rate and vorticity; each has been normalised by the corresponding value for the freely-propagating flame, apart from the vorticity, which has been normalised by the peak value on the unburned side of the control flame.

The top row shows the control flame, which presents the usual thermodiffusively-unstable characteristics; the flame burns with a cellular structure, with high fuel consumption associated with regions of positive curvature (with the centre of curvature in the products) resulting in hot-spots where the temperature exceeds that of the adiabatic flame temperature (see [1, 10] for more details).

The second row shows the simulation where all of the species diffusion coefficients have been equated with that of molecular hydrogen. It is clear that there is little visual difference between this case and the control. A similar flame response is found when all of the species except $H_2$ have unity Lewis number; there is little visual difference between this case and the control, and almost no difference with case Ib.

Case Id is shown in the fourth row, where the Lewis number for $H_2$ is taken to be unity, with all of the other species unchanged. The difference between this case and the previous three is substantial. The super-adiabatic regions are no longer present, the cellular burning is no longer apparent, and the fuel consumption has dropped significantly, and presents little if any variation along the flame surface.

Setting all of the species to have unity Lewis number, case Ie on the penultimate row, presents a similar flame response to case Id; the signatures of the thermodiffusive instability are not present, and the fuel consumption appears to be higher than in case Id, but again presents little variability along the flame surface.

The final case, bottom row, exaggerates the thermodiffusive instability by reducing the thermal diffusion by an order of magnitude. Here the cellular burning is recovered, and the structure size appears to be smaller than cases Ia-c. Most noticeably, the post-flame region has a higher temperature variation, and further exceeds the adiabatic flame temperature.

The visual effects presented in figure 1 can be quantified by considering the correlation of a consumption-based local flame speed with the curvature at the flame surface. To compute this quantity, the flame surface was identified with the 1330 K isotherm, which is the temperature corresponding to peak fuel consumption. A local coordinate system is then constructed in a neighbourhood of the flame by

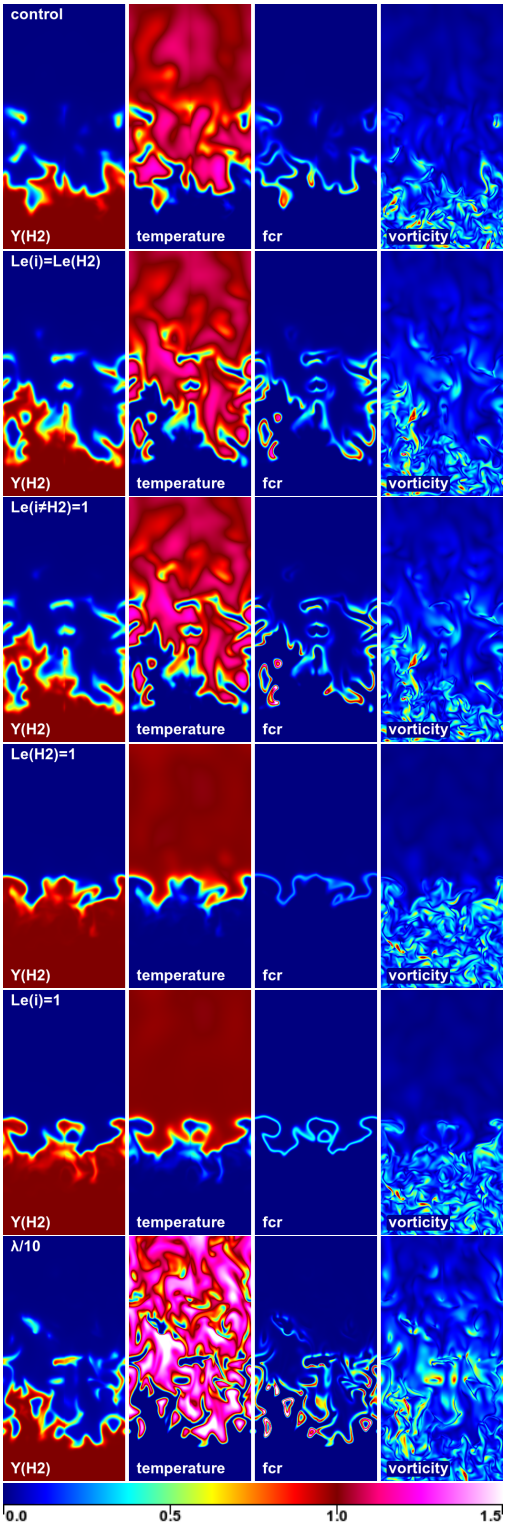


Fig. 1: Two-dimensional slices through the three-dimensional simulations with modified diffusion coefficients.

following integral curves of $\nabla T$, following the procedure detailed in [19]. Given a fine triangularisation of the flame surface, a prism (with triangular cross section) can be constructed extending from the triangle that follows the local coordinate lines in both directions. Integration of the fuel consumption over these prisms allows a local consumption-based flame speed to be defined,

$$s_T^c = \frac{1}{(\rho Y_{\mathrm{H}_2})_{\mathrm{reac}} A_{\mathrm{ref}}} \int_\Omega \rho \dot{\omega}_{\mathrm{H}_2} \, \mathrm{d}\Omega, \qquad (4)$$

where the suffix reac denotes the reactants, $\Omega$ is prism volume, and $A_{\mathrm{ref}}$ is the area of intersection between the $\Omega$ and the flame surface.

The joint probability density functions (JPDFs) of this consumption-based local flame speed and mean curvature are shown in figure 2 for the six cases Ia-If; note the first moment with respect to flame speed has been plotted to reduce the influence of the local extinction regions (specifically, $s_T^c p(M, s_T^c)$ has been plotted, where $p(M, s_T^c)$ is the JPDF, and $M$ is the mean curvature), the curvature and flame speed have been normalised by the flame thickness and speed of the freely-propagating flame, respectively. The positive correlation observed in figure 1 for cases Ia-Ic is clearly apparent here. There are subtle differences between the three cases; specifically, compared with case Ia, the correlation is slightly steeper for case Ib and slightly shallower for case Ic. Cases Id and Ie, where the global Lewis number has been set to unity present starkly different JPDFs. The flame speeds are much lower than $s_F$ and the correlation is much flatter than the previous three cases, but still appears to be positive (interestingly in contrast to the global unity Lewis number flames presented in [6]). Finally, the case with reduced thermal diffusion appears to have a positive correlation but a greater variation than all of the other cases.

The global Lewis number appears to dominate the diffusion of all of the other species at these conditions and is responsible for the leading order flame response to turbulence. There are some subtle differences associated with diffusion of the other species, but these are much less pronounced.

### *3.2. Part II: atomic hydrogen diffusion*

Two-dimensional slices for cases IIa and IIb are shown in figure 3, where the panels (left-to-right) are fuel mass fraction, temperature, fuel consumption rate, heat release and atomic hydrogen mass fraction; all panels have been normalised by the appropriate value in the freely-propagating flame, and again, periodicity has been exploited to stitch together $x = 0$ and $y = 0$ planes to show more flame surface (each panel is two domain widths across and 2.67 domain widths high).

At first glance, the two simulations appear to be almost identical, especially the fuel and temperature fields. Upon closer inspection, differences can be found, especially in the fuel consumption rate, heat

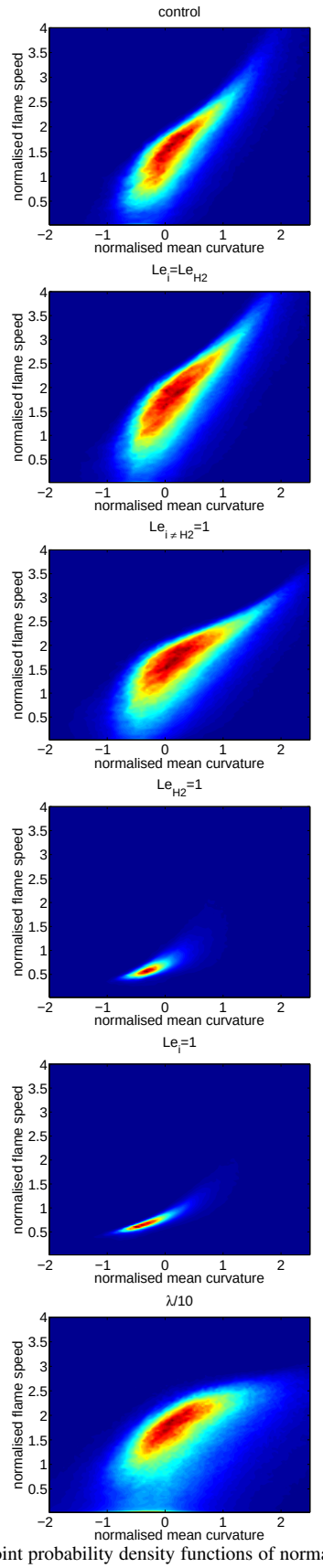


Fig. 2: Joint probability density functions of normalised local consumption-based flame speed and normalised mean curvature.

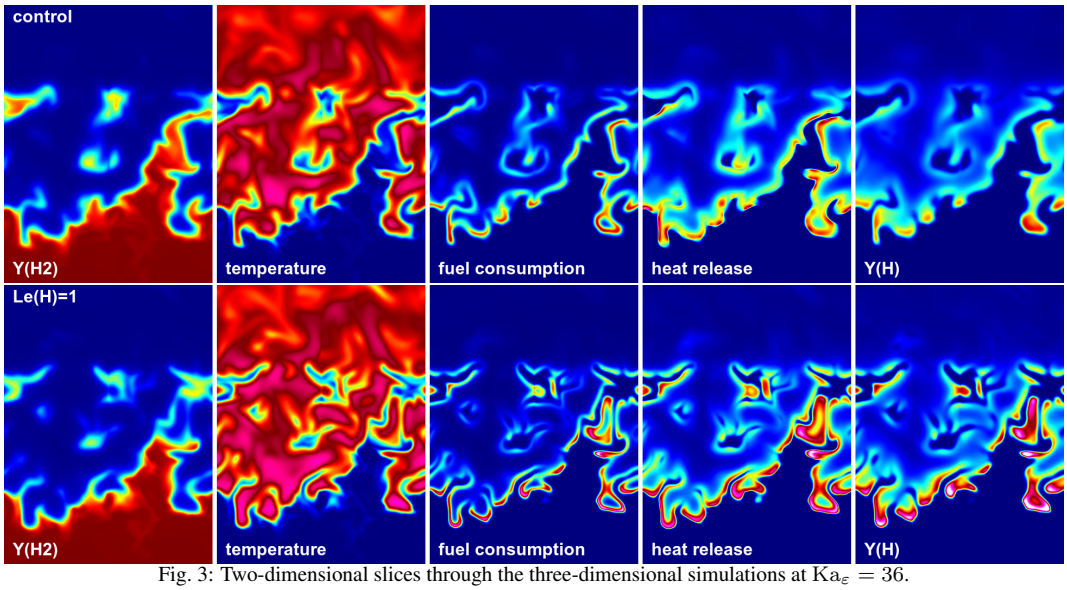

Fig. 3: Two-dimensional slices through the three-dimensional simulations at $\mathrm{Ka}_\varepsilon = 36$.

release and atomic hydrogen mass fraction, which are all found to attain higher values than the freely propagating flame (as indicated by magenta and white patches). Note, in particular, how the decorrelation between fuel consumption rate and heat release reported in [10] has (naturally) been recovered in the control (case Ia), but appears not to be present in the simulation with unity Lewis number transport for atomic hydrogen (case IIb). Furthermore, note how the atomic hydrogen appears thinner, but also in higher concentrations, leading to an accompanying increase in reactions rates (as shown by the magenta and white regions, which indicate values over ten times the steady unstrained flat flame values).

The JPDF of heat release and fuel consumption rate is presented in figure 4 and highlights the stark difference between the two simulations. In the control, the decorrelation is clear; there is high heat release where the fuel consumption rate remains low. In the case with unity Lewis number transport of atomic hydrogen, the correlation along with the elevated values that are attained is clear.

Changing the transport property of a single (secondary) species has a clear and pronounced effect on the turbulent flame response; the decorrelation of fuel consumption rate and heat release at high positive curvature as observed in [10] can be attributed to the high mobility of atomic hydrogen. The decorrelation appears to result in regions of high positive curvature where molecular hydrogen diffuses into small pockets of heat, resulting in high levels of fuel consumption, producing high levels of atomic hydrogen, which in turn diffuse away due to the low Lewis number, and the heat release occurs away from the region of fuel consumption.

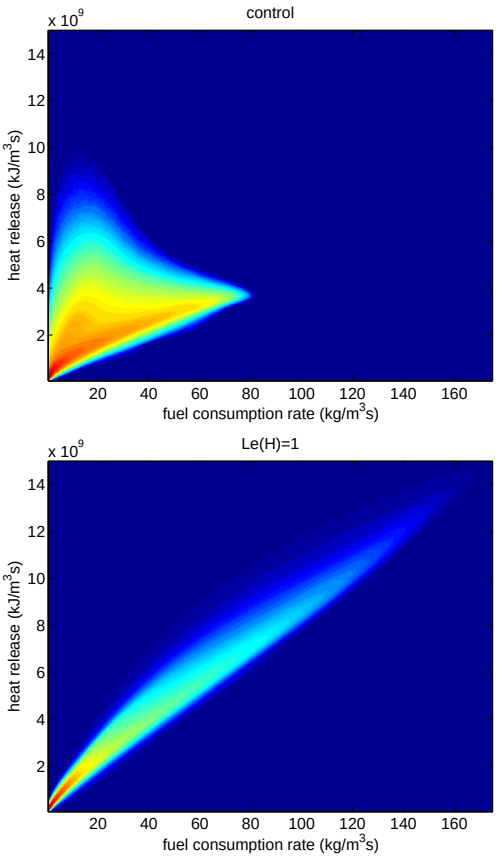

Fig. 4: Joint probability density functions of heat release and fuel consumption rate.

*3.3. Part III: viscosity*

Two-dimensional slices through the three-dimensional data are presented in figure 5 for the seven cases cases IIIb-IIIh, case IIIa is the same as case Ia (top row of figure 1); again all fields are normalised by the corresponding value in the freely-propagating flame, and vorticity is normalised by the same value in each case, taken from the control case. The apparent flame structure (fuel, temperature and burning rate) of the four cases with constant viscosity (top four rows, cases IIIb-IIIe) appears to be similar to the control case (figure 1), and the turbulence appears to be greatly reduced in the post flame region. Visually, the suppression of turbulence cannot be attributed to the increase in viscosity as a result of the increase in temperature through the flame. Allowing the viscosity to decrease across the flame (cases IIIc,d), appears to lead to a decrease in turbulence close to the flame, but the vorticity increases further from the flame (resulting from a combination of shear and baroclinic torque). Setting the viscosity to zero across the whole flame (case IIIg in the penultimate row) leads to significant turbulence in the fuel region (hence the motivation for running case IIIe), which experiences a change in distribution through the flame, but is not suppressed to the same extent as cases IIIa-d. Finally, the ILES case (bottom row) presents very different behaviour; scalar mixing is occurring due to numerical diffusion and the flame bears little resemblance to a real premixed flame. ILES is naturally not recommended for turbulent premixed combustion; flames are fundamentally driven by thermal or species diffusion, which cannot be recovered with inherent numerical dissipation. It should be noted that the supernovae simulations of [20, 21] were driven by optically-thick radiation, which was included explicitly, and were not pure ILES.

To examine the turbulent properties through the flame, spatial and temporal averaging has been performed. Integrating to find the total mass of fuel in the domain and dividing by the fuel density times the cross-section area gives a flame position $z_0(t)$, which allows a normalised coordinate to be defined as $\eta(t) = (z - z_0)/l_F$. Averaging was then performed spatially in each $z$ plane and temporally using $\eta$ as a local coordinate from the flame. The averaged enstrophy is plotted in figure 6; note that each case was normalised by the spatial average over the region $\eta \in [-15, -5]$ to give the relative change through the flame. The control case (black) presents the most significant decrease in enstrophy across the flame, down to a few percent of the pre-flame value. The three cases with constant dynamic viscosity (red) also present significant decrease across the flame (down to less than 10%), and even the cases where the viscosity decreases in the post-flame (blue and magenta) present a drop of over 60% in enstrophy.

While the suppression of turbulence cannot be attributed to the increase in viscosity across the flame, there is a secondary effect due to increasing viscosity

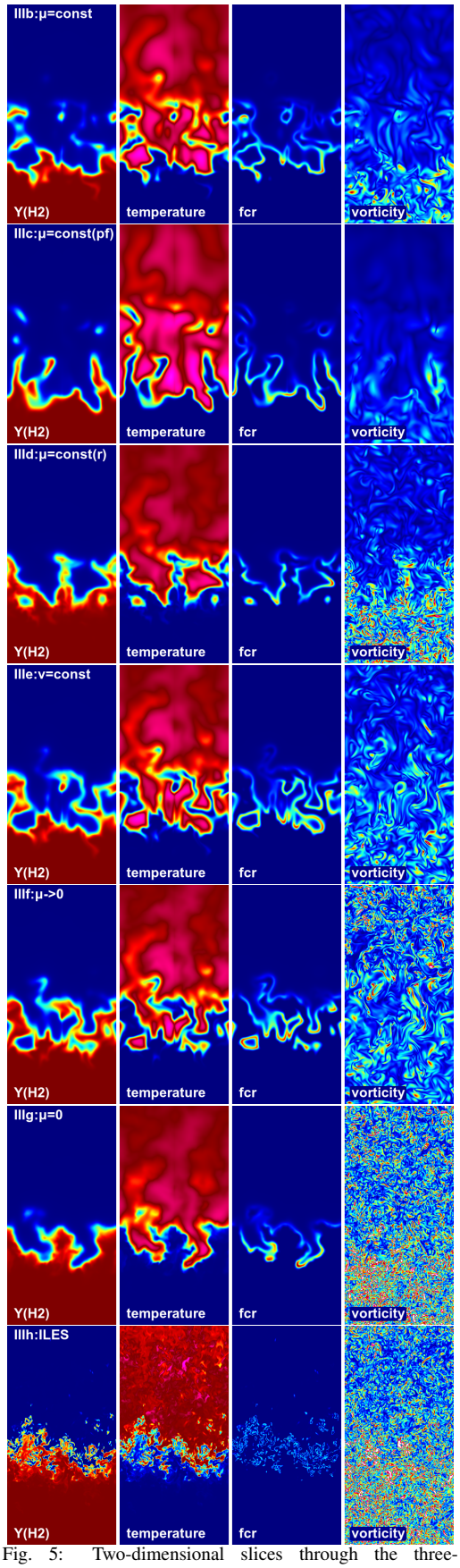


Fig. 5: Two-dimensional slices through the three-dimensional simulations with modified viscosity (pf and r denote post-flame and reduced, repsectively).

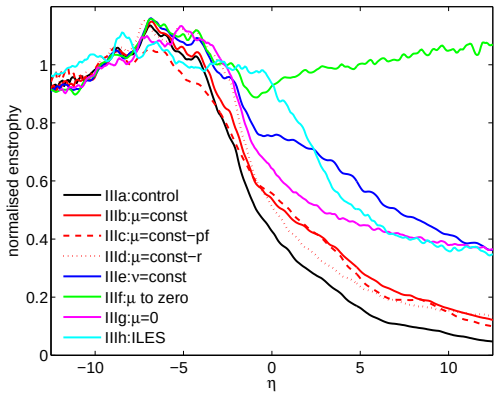


Fig. 6: Normalised enstrophy through the flame for cases IIIa-IIIh; $\eta = (z - z_0)/l_F$ is a normalised distance from the average flame position.

with temperature.

## 4. Conclusions

A variety of turbulent lean premixed hydrogen flames have been simulated with artificial modifications to the diffusive transport properties. The global Lewis number (the Lewis number of the deficient species) has been shown to be the dominant factor in determining the turbulent flame response, with little influence from the other species. The decorrelation of fuel consumption and heat release at higher Karlovitz numbers reported in [9, 10] has been attributed solely to the diffusion of atomic hydrogen; atomic hydrogen is able to diffuse upstream and, as suggested by [9] and observed in [10], enhance the heat release from the recombination reaction H+$O_2$+M=$HO_2$+M. Indeed, the diffusion of atomic hydrogen was shown in [6] to have secondary effects in methane flames similar to those presented in section 3.1; specifically, if it wasn't for the high mobility of atomic hydrogen, premixed flames would be much thinner with higher reaction rates. It has also been shown that the suppression of turbulence through the flame cannot be attributed to an increase in viscosity due to the increase in temperature, but that the effect is not negligible. The Author speculates that it is the fluid expansion through the flame that is the primary mechanism for the suppression of turbulence, and will be the subject of future work. It is interesting to note that changes to viscosity made little difference to the general stucture and appearance of the flame; again, the global Lewis number is more important. Consequently, this lends support to defining the Karlovitz number following equation (3) rather than equation (2) as it is representative of the inertial subrange rather than the dissipation subrange.

## Acknowledgements

The Author would like to thank John Bell, Marc Day, Ed Richardson and Bruno Savard for many useful discussions, and to acknowledge the use of the IRIDIS High Performance Computing Facility and associated support services at the University of Southampton.

## References

[1] A. J. Aspden, M. S. Day, J. B. Bell, *Journal of Fluid Mechanics* 680 (2011) 287–320.
[2] B. Savard, G. Blanquart, *Combustion and Flame* 161 (6) (2014) 1547–1557.
[3] H. Carlsson, R. Yu, X.-S. Bai, *International Journal of Hydrogen Energy* 39 (35) (2014) 20216–20232.
[4] H. Carlsson, R. Yu, X.-S. Bai, *Proceedings of the Combustion Institute* 35 (2) (2015) 1425–1432.
[5] B. Yenerdag, Y. Naka, M. Shimura, M. Tanahashi, in: *Interntational Symposium on Turbulence and Shear Flow Phenomenon*, 2015.
[6] A. J. "Aspden, M. S. Day, J. B. Bell, *Combustion and Flame* 166 (2016) 266–283.
[7] B. Savard, B. Bobbitt, G. Blanquart, *Proceedings of the Combustion Institute* 35 (2) (2015) 1377–1384.
[8] A. J. Aspden, J. B. Bell, M. S. Day, F. N. Egolfopolous, *accepted to the Combustion Symposium*.
[9] J. B. Chen, H. G. Im, *Proceedings of the combustion institute* 28 (1) (2000) 211–218.
[10] A. J. Aspden, M. S. Day, J. B. Bell, *Proceedings of the Combustion Institute* 35 (2) (2015) 1321 – 1329.
[11] N. Peters, *Turbulent Combustion*, Cambridge University Press, 2000.
[12] A. J. Aspden, M. S. Day, J. B. Bell, *Proceedings of the Combustion Institute* 33 (1) (2011) 1463–1471.
[13] S. G. Saddoughi, S. V. Veeravalli, *Journal of Fluid Mechanics* 268 (1994) 333–372.
[14] A. J. Aspden, N. Nikiforakis, S. B. Dalziel, J. B. Bell, *Comm. App. Math. Comput. Sci.* 3 (1) (2008b) 101.
[15] M. S. Day, J. B. Bell, *Combust. Theory Modelling* 4 (2000) 535–556.
[16] J. Li, Z. Zhao, A. Kazakov, F. L. Dryer, *International Journal of Chemical Kinetics* 36 (10) (2004) 566–575.
[17] T. Poinsot, D. Veynante, *Theoretical and numerical combustion*, RT Edwards, Inc., 2005.
[18] F. F. Grinstein, L. G. Margolin, W. J. Rider, *Implicit Large Eddy Simulation*, Cambridge University Press, 2007.
[19] M. S. Day, J. B. Bell, P.-T. Bremer, V. Pascucci, V. Beckner, M. J. Lijewski, *Combustion and Flame* 156 (5) (2009) 1035 – 1045.
[20] A. J. Aspden, J. B. Bell, M. S. Day, S. E. Woosley, M. Zingale, *The Astrophysical Journal* 689 (2008) 1173–1185.
[21] A. J. Aspden, J. B. Bell, S. E. Woosley, *The Astrophysical Journal* 710 (2010) 1654–1663.